

Systematic Structural Determinants of the Effects of Tetraphosphonates on Gypsum Crystallization

Emel Akyol,[†] Mualla Öner,^{*†} Eleni Barouda,[‡] and Konstantinos D. Demadis^{*,‡}

[†]Department of Chemical Engineering, Yildiz Technical University, Davutpasa, Istanbul, 34210, Turkey, and [‡]Crystal Engineering, Growth and Design Laboratory, Department of Chemistry, University of Crete, P.O. Box 2208, Voutes Campus, Heraklion, Crete, GR-71003, Greece

Received May 20, 2009; Revised Manuscript Received October 20, 2009

ABSTRACT: In this study, the effect of phosphonate additives on the crystallization of calcium sulfate dihydrate ($\text{CaSO}_4 \cdot 2\text{H}_2\text{O}$, gypsum) has been investigated in aqueous solutions. Ethylenediamine-tetrakis(methylenephosphonic acid) (EDTMP), hexamethylenediamine-tetrakis(methylenephosphonic acid) (HDTMP), octamethylenediamine-tetrakis(methylenephosphonic acid) (ODTMP), and dodecamethylenediamine-tetrakis(methylenephosphonic acid) (DDTMP) have been used as additives. It was found that they are very effective retardants for the crystallization of calcium sulfate dihydrate. The inhibition efficiency is directly proportional to the number of methylene groups in the organic chain that connects the amino-bis(methylenephosphonate) moieties. The degree of inhibition of crystallization was measured as an increase in induction time and reduction in crystallization rate. Particle size and crystal morphology were determined with a particle-sizer and scanning electron microscopy. According to experimental results, phosphonate additives tested in this study are very effective retardants for the formation of calcium sulfate dihydrate scale. The crystal structure of $[\text{Ca}(\text{EDTMP})(\text{H}_2\text{O})_2] \cdot \text{H}_2\text{O}$ is also reported. This is a one-dimensional coordination polymer in which EDTMP acts as both a bidentate chelate and a bridge for Ca^{2+} centers.

Introduction

The crystallization of $\text{CaSO}_4 \cdot 2\text{H}_2\text{O}$ (gypsum) has been widely studied due to its importance in many technologies, such as desalination,¹ water treatment,² geothermal and oil-field drilling,³ and phosphoric acid production.⁴ The formation of tenaciously adhering calcium sulfate scale in a number of processes from water desalination to heat exchangers and processes involving heating of water is a persistent problem. Scaling reduces heat transfer effectiveness over time, leading to unacceptable heat transfer rates. Methods of preventing scale formation are therefore desirable.^{5–10}

Several scale mitigation strategies have been proposed.¹¹ A widely used approach for controlling the scale deposition is the addition of scale inhibitors to the feedwater. Scale inhibitors are “small” organic molecules or anionic polymers.^{2b,12} The retardation mechanisms of precipitation in the presence of impurities are very complicated, but the most widely accepted view for the retardation of precipitation is that impurities adsorb on the growth sites of forming nuclei, thus preventing their further growth.¹³ A number of additives have been found to be efficient inhibitors in preventing or reducing the rate of precipitation of calcium sulfate from supersaturated solutions.¹⁴ Recently, there has been an increasing interest in the application of phosphonates as crystallization inhibitors, since these are highly efficient in preventing the nucleation and crystallization of many sparingly soluble inorganic salts.^{2,15} They can also augment in influencing the adherence of inorganic crystals onto critical system surfaces.¹⁶ From a practical point of view, the use of phosphonates in controlling scale formation has certain advantages because of their excellent inhibitory efficiency, but also due to their high stability even at relatively high temperature¹⁷ and harsh conditions.¹⁸

This work focuses on the investigation of a family of additives containing four phosphonic acid groups and mapping of their relative effectiveness in inhibiting the crystal growth of calcium sulfate dihydrate. These tetraphosphonates share a common structural feature, that each phosphonate group is attached to an N atom via a methylene moiety ($\text{N}-\text{CH}_2-\text{PO}_3\text{H}_2$). Therefore, each side of the phosphonate additive has two methylenephosphonate groups connected to an N atom. Finally, the two N atoms are connected by a number of methylene groups (2, 4, 6, 8, and 12), depending on the additive. The structures of the tetraphosphonates are shown in Scheme 1.

Experimental Section

Crystal growth experiments were carried out in a water-jacketed Pyrex glass of 1 L capacity at 30 ± 0.1 °C. Supersaturated solutions for crystal growth experiments were prepared by slow mixing of equal volumes (0.12 M) of calcium chloride dihydrate ($\text{CaCl}_2 \cdot 2\text{H}_2\text{O}$, Merck) and sodium sulfate (Na_2SO_4 , Sigma-Aldrich) solutions. The additives EDTMP, HDTMP, ODTMP, and DDTMP were used to retard the growth rate of gypsum. Scheme 1 shows their schematic chemical structures. These phosphonates were synthesized according to literature procedures.¹⁹

The freshly prepared additive solutions were added to the reaction medium together with the sulfate solution. $[\text{Ca}^{2+}]$, pH, and temperature of the reaction solutions were monitored by personal computer during crystallization. The experimental procedure has been reported previously in detail.^{20,21} The effect of additives on the precipitation rate of calcium sulfate was evaluated by recording the decrease in $[\text{Ca}^{2+}]$ as a function of time. The precipitation process, and the concurrent decrease in calcium activity as a function of time, were monitored and quantified by means of a Radiometer Impulsomat (PHM290) using the Ca-ISE electrode (Radiometer, ISE-K-CA).

The course of the some selected experiments was also followed by removing homogeneous aliquots at various times and quickly filtered through Millipore filters of 0.22 μm pore size. The aqueous phase was analyzed for calcium by atomic absorption spectroscopy (Perkin-Elmer AAnalyst 200). The measurement was consistent with the computer monitored activities.

*Corresponding authors. E-mail: (M.O.) oner@yildiz.edu.tr; (K.D.D.) demadis@chemistry.uoc.gr.

Scheme 1. Additives Used in This Work and Their Schematic Structures

Additive abbreviation	Additive Name	Additive Schematic Structure
EDTMP (C ₂)	Ethylenediamine- <i>tetrakis</i> (methylenephosphonic acid)	
HDTMP (C ₆)	Hexamethylenediamine- <i>tetrakis</i> (methylenephosphonic acid)	
ODTMP (C ₈)	Octamethylenediamine- <i>tetrakis</i> (methylenephosphonic acid)	
DDTMP (C ₁₂)	Dodecamethylenediamine- <i>tetrakis</i> (methylenephosphonic acid)	

CaSO₄ crystal morphologies and sizes were investigated by using SEM (JEOL-FEG-SEM) and particle sizer (Fritsch Standart F500). The effect of additives can be quantified as the ratio of the rate of crystallization of the pure solution (R_0 , mg/L min) to the rate of crystallization in the presence of additive (R_i , mg/L min) at the same concentration and temperature. The rates reported were the initial rapid growth rate calculated from slope of the calcium ion potential-time plots for each experiment. The time between the generation of a supersaturated state and the first observed change in calcium ionic activity was defined as the induction period (t_{ind}). The time periods were determined from at least three separate experiments and only the average values were reported. The reproducibility of this technique was ~4–5%.

Synthesis of [Ca(EDTMP)(H₂O)₂]·H₂O (Ca-EDTMP). EDTMP acid (1.50 mmol, 0.71 g) was suspended in ~40.0 mL of in-house deionized water. Using a 1.0 M NH₄OH stock solution, the pH was adjusted to ~4.0 and the solid was dissolved. To that clear and colorless solution a quantity of the hydrated calcium chloride (1.50 mmol, 0.40 g, molar ratio 1:1) was gradually added as a solid under constant stirring. The pH dropped, but was readjusted with a 1.0 M stock solution of NH₄OH to ~4.0. The homogeneous solution was left at quiescent conditions. After several days, single crystals of Ca-EDTMP appeared. Crystal growth was allowed to proceed for

2 weeks. The product was collected by filtration and air-dried. Typical yields are ~50%. Complete spectroscopic and thermal characterization of this material can be found in the Supporting Information.

Crystallography. X-ray diffraction data were collected on a SMART 1K CCD diffractometer at 298(2) K with Mo K α ($\lambda = 0.71073$ Å). Crystal and refinement data are presented in Table 1. Copies of crystallographic data for the structure may be obtained free of charge from CCDC by quoting the reference number 605561 for [Ca(EDTMP)(H₂O)₂]·H₂O.

Results and Discussion

The aim of this study was quantification and comparison of the systematic effects of various additives containing phosphonic acid groups on calcium sulfate crystallization. Four tetraphosphonates have been investigated under identical growth conditions. These tetraphosphonates contain two -N(CH₂PO₃H₂)₂ moieties, but the polymethylene linker that connects the N atoms has systematically variable length ((-CH₂)_x-, $x = 2, 6, 8, 12$). The measurement of nucleation rate is not trivial. An accepted method to evaluate the effect of

Table 1. Crystal Data and Structure Refinement for Ca[(EDTMP)-(H₂O)₂]₂·H₂O (Ca-EDTMP)

Ca[(EDTMP)(H ₂ O) ₂] ₂ ·H ₂ O	
empirical formula	C ₆ H ₂₄ CaN ₂ O ₁₅ P ₄
formula weight	528.24
temperature (K)	298(2)
wavelength (Å)	0.71073
crystal system	monoclinic
space group	C2/c
unit cell dimensions	
<i>a</i> (Å)	13.206(3)
<i>b</i> (Å)	10.368(2)
<i>c</i> (Å)	13.763(3)
α (deg)	90.00
β (deg)	97.367 (18)
γ (deg)	90.00
volume (Å ³)	1868.9 (7)
<i>Z</i>	4
density (calc) (g·cm ⁻³)	1.877
absorption coefficient (mm ⁻¹)	0.758
<i>F</i> (000)	1096
crystal size (mm)	0.11 × 0.08 × 0.05
θ range for data collection (deg)	2.51 to 28.06
index ranges	-16 ≤ <i>h</i> ≤ 16, -7 ≤ <i>k</i> ≤ 13, -16 ≤ <i>l</i> ≤ 17
reflections collected	5926
independent reflections	2099 [<i>R</i> (int) = 0.0251]
independent reflections [<i>I</i> > 2 σ (<i>I</i>)	1766 [<i>R</i> (int) = 0.0248]
refinement method	full-matrix least-squares on <i>F</i> ²
data/restraints/parameters	2099/0/141
goodness-of-fit on <i>F</i> ²	1.077
final <i>R</i> indices [<i>I</i> > 2 σ (<i>I</i>)	<i>R</i> 1 = 0.0362, <i>wR</i> 2 = 0.1052
<i>R</i> indices (all data)	<i>R</i> 1 = 0.0439, <i>wR</i> 2 = 0.1094
largest diff peak and hole (e ⁻ ·Å ⁻³)	0.494 and -0.384

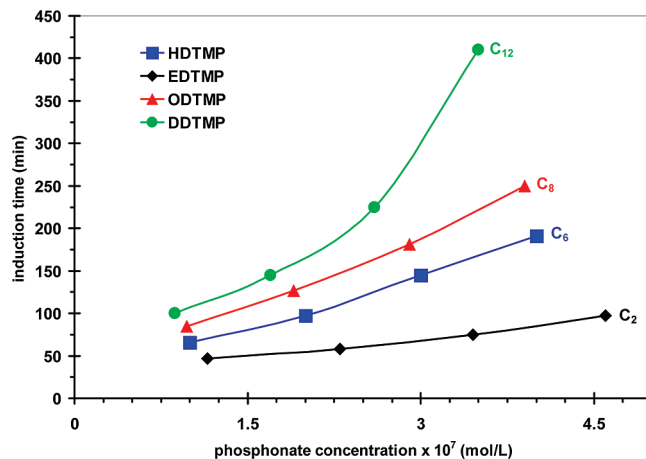
Table 2. The Effect of Additives on Calcium Sulfate Crystallization

polymer	concentration × 10 ⁷ (M)	<i>t</i> _{ind} (min)	<i>R</i> ₀ / <i>R</i> _{<i>i</i>}
control		47	1.0
EDTMP	1.2	47	1.0
	2.3	58	1.0
	3.5	75	1.2
	4.6	97	1.3
	11.5	^a	^a
HDTMP	1.0	66	1.2
	2.0	97	1.1
	3.0	145	1.1
	4.0	191	1.2
	10.0	^a	^a
ODTMP	0.9	85	1.0
	1.9	127	1.1
	2.9	181	1.2
	3.9	250	1.2
	9.0	^a	^a
DDTMP	0.9	100	1.0
	1.7	145	1.0
	2.6	225	1.1
	3.5	410	1.3
	8.7	^a	^a

^aNo crystallization.

additives on nucleation is to measure their abilities to affect the induction time (*t*_{ind}). This is defined as the time between the generation of a supersaturated state and the first observed change in calcium concentration. The ability of additives to act as inhibitors was evaluated by *t*_{ind} and *R*₀/*R*_{*i*} ratios. Higher *t*_{ind} and *R*₀/*R*_{*i*} values indicate more effective inhibition. Table 2 summarizes the additives used in this study and the effect of additives on crystallization.

As shown in Table 2, all additives lead to temporary inhibition of calcium sulfate growth from its supersaturated solution. The induction period is much more sensitive to changes in tetraphosphonates concentration. Although the

**Figure 1.** Effect of additive concentration on calcium sulfate crystallization.

rate of crystallization is marginally affected at additive concentrations of below 9.0×10^{-7} mol/L, all tetraphosphonates at a concentration of 9.0×10^{-7} mol/L can completely inhibit crystallization over an 8 h period, which indicated a dramatic effect on induction time. Figure 1 indicates that an increase in additive concentration results in a *t*_{ind} increase. This means that the duration of the induction period is increased by increasing additive concentration. When we compare the effect of additives on calcium sulfate dihydrate crystallization, the retardation ranking is DDTMP > ODTMP > HDTMP > EDTMP.

These results demonstrate that inhibition efficiency increases proportionally to the number of methylene groups linking the two N atoms (see Scheme 1). It is also interesting to note that the crystallization reaction following the initial induction period takes place at a rate comparable to the rate of crystallization from pure solution for all additives. This phenomenon has been discussed by Liu and Nancollas,¹⁷ who attributed this stabilization action to an increase in the energy of the formation of the critical nuclei as a result of the endothermal adsorption of the additive on the surface of the nucleus. This model, which requires a high mobility of the adsorbed inhibitor ions along the crystal surface yields a comparatively low value for the surface coverage needed to accomplish growth blockage. If the inhibitor ions are rapidly adsorbed, the nuclei remain subcritical and disappear. The inhibitor ions are then available for repeated adsorption at the edges of newly developing nuclei. This eventually leads to breakdown and disintegration of a number of available embryos before further growth can take place. In this way, outgrowth of the nuclei beyond their critical value is hampered; in due course, because of their thermodynamic instability, most nuclei would redissolve, thus freeing up the additives. The changes in solution concentration during this stage may be too small to be detected. Therefore, the adsorbed additives retard crystal growth temporarily, but they soon desorb and the growth can resume at a rate comparable to that of the unpoisoned system.²² This sequence of additive adsorption and desorption contributes to intermittent inhibition. This subject area undoubtedly needs more research.

Since the amounts of additive in solution are small, the growth inhibition is most likely caused by additive adsorption of the active growth sites on crystal surfaces. However, calcium-phosphonate complex formation cannot be ruled out. Such metal-inhibitor complexes were found to promote inhibition of barite (BaSO₄).^{15b,23}

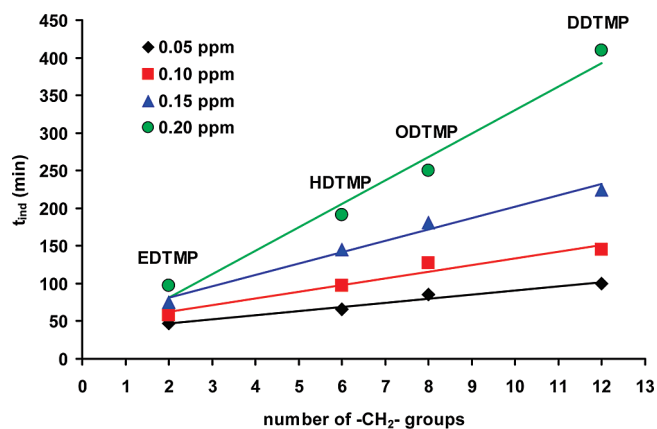


Figure 2. Linear dependence of t_{ind} on the length of the phosphonate additive.

Table 3. Equilibria and Complexation Reactions Occurring During Gypsum Crystallization in the Presence of EDTMP (= L)^{25–27}

equilibrium	log K
$\text{Ca}^{2+} + \text{SO}_4^{2-} = \text{CaSO}_4^0$	-2.31
$\text{Na}^+ + \text{SO}_4^{2-} = \text{NaSO}_4^-$	-0.7
$\text{H}^+ + \text{SQ}^{2-} = \text{HSO}_4^-$	1.99
$\text{L}^{2-} + \text{H}^+ = \text{HL}^{7-}$	12.99
$\text{HL}^{7-} + \text{H}^+ = \text{H}_2\text{L}^{6-}$	9.78
$\text{H}_2\text{L}^{6-} + \text{H}^+ = \text{H}_3\text{L}^{5-}$	7.94
$\text{H}_3\text{L}^{5-} + \text{H}^+ = \text{H}_4\text{L}^{4-}$	6.42
$\text{H}_4\text{L}^{4-} + \text{H}^+ = \text{H}_5\text{L}^{3-}$	5.17
$\text{H}_5\text{L}^{3-} + \text{H}^+ = \text{H}_6\text{L}^{2-}$	3.02
$\text{H}_6\text{L}^{2-} + \text{H}^+ = \text{H}_7\text{L}^-$	1.33
$\text{Ca}^{2+} + \text{L}^{8-} = \text{CaL}^{6-}$	9.36
$\text{H}^+ + \text{CaL}^{6-} = \text{CaHL}^{5-}$	9.42
$\text{H}^+ + \text{CaHL}^{5-} = \text{CaH}_2\text{L}^{4-}$	8.44
$\text{H}^+ + \text{CaH}_2\text{L}^{4-} = \text{CaH}_3\text{L}^{3-}$	6.59
$\text{H}^+ + \text{CaH}_3\text{L}^{3-} = \text{CaH}_4\text{L}^{2-}$	5.25
$\text{CaSO}_4 \cdot 2\text{H}_2\text{O}(\text{s}) = \text{Ca}^{2+} + \text{SO}_4^{2-} + 2\text{H}_2\text{O}$	-4.92

Table 4. Experimental Conditions for the Crystallization of Gypsum at Different Supersaturations ($T = 30^\circ\text{C}$, 0.05 mg/L EDTMP)

$\text{Ca}_T \times 10^2$ (mol/L)	R (mol/L·min)	t_{ind} (min)	σ
6	2×10^{-4}	47	0.979
7	3×10^{-4}	30	1.180
8	5×10^{-4}	18	1.377
9	8×10^{-4}	13	1.564
10	1×10^{-3}	11	1.748

In Figure 2 plots of t_{ind} vs the number of methylene groups ($-(\text{CH}_2)_x-$, $x = 2, 6, 8, 12$) separating the N atoms (and by inference the phosphonate moieties) are shown. It is clear that there is a linear dependence of t_{ind} on x .

The crystal growth rates, R , were determined as (mol/L·min) from spontaneous experiments. The relative solution supersaturation with respect to gypsum, σ , is defined as

$$\sigma = \frac{\text{IP}^{1/2} - K_{sp}^{1/2}}{K_{sp}^{1/2}} = S^{1/2} - 1 \quad (1)$$

in which IP is the ionic activity product and K_{sp} represents the thermodynamic solubility product. They are summarized in Table 3. The ratio IP/K_{sp} represents the degree of supersaturation, S , and was computed by using MINEQL+ chemical equilibrium modeling software,²⁴ which is a free energy minimization program taking into account all equilibria in the solution, mass balance, and electroneutrality conditions. The values of the thermodynamic solubility product (K_{sp}) and association constant of ions were obtained from the literature.^{25–27} The calculated growth rates and relative supersaturations are given in Table 4.

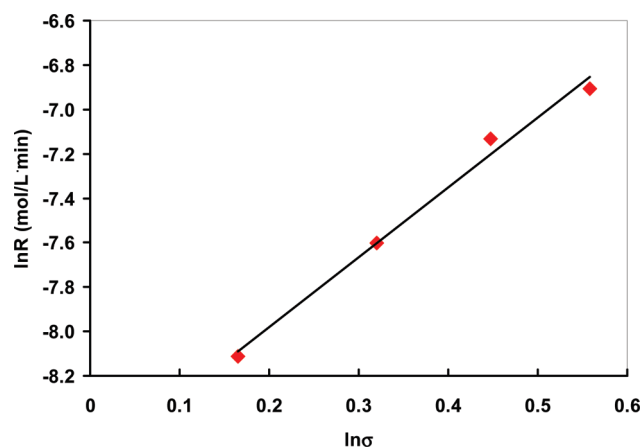


Figure 3. Logarithmic plot of rate of precipitation of gypsum vs the relative solution supersaturation.

The rate of gypsum crystallization can be expressed in terms of semiempirical kinetics equation:

$$R = k\sigma^n \quad (2)$$

where k is the rate constant for crystal growth, and n is the apparent order of the crystal growth.

Logarithmic plots of the rates of gypsum formation on gypsum crystals as a function of the relative supersaturation yielded a straight line as shown in Figure 3.

The value of n , the effective order of the reaction, is calculated from the slope of the line. The effective order of the reaction was found as 3.1 for gypsum growth in the presence of 0.05 mg/L EDTMP. This dependence is indicative of a “polynuclear layer” surface reaction-controlled growth²⁸ as originally proposed by Nielsen.²⁹

The kinetics and mechanism of calcium sulfate crystallization have been studied extensively over the years by a number of researchers. Despite this growing body of literature, there is significant uncertainty regarding the order of the crystal growth kinetics. Schierholts conducted spontaneous crystallization studies by mixing equimolar amounts of calcium hydroxide and sulfuric acid at 10°C , and raised the experiment temperature of the solution to 25°C whereby precipitation occurred.³⁰ Schierholts reported a first-order growth rate, $n = 1$, suggesting diffusion controlled growth, but the plot of his experimental results showed considerable deviations from linearity. McCartney and Alexander’s results gave second-order plots for part of the crystallization range.³¹ Packter conducted homogeneous crystallization experiments using equivalent calcium nitrate solution and sodium sulfate solutions at 0.02 to 0.24 M under constant stirring at 100 rpm at 22°C and obtained a rate order of $n = 9–10$.³² Nancollas argued that spontaneous crystallization studies conducted using the above method for sparingly soluble salts were difficult to reproduce and demonstrated that by using the seeded growth technique for gypsum crystallization, excellent reproducibility was obtained suggesting that $n = 2$.³³ Tadros and Mayes studied the structure of forming gypsum crystals with Polaroid photomicrographs, in the presence of carboxylic and phosphonic acid derivatives, by mixing sodium sulfate and calcium chloride.³⁴ They concluded that gypsum crystallization followed second order with respect to concentration ($n = 2$), which they suggested was indicative of a polynuclear layer reaction-controlled growth mechanism. Klepetsanis and Koutsoukos studied precipitation of calcium sulfate dihydrate at constant activity.³⁵ The kinetics of

precipitation was found to be independent of pH, and order of reaction of $n = 4$ for the precipitation process was found from the kinetics based on the initial rates. He et al. studied the seeded crystal growth rate of calcium sulfate dihydrate.³⁶

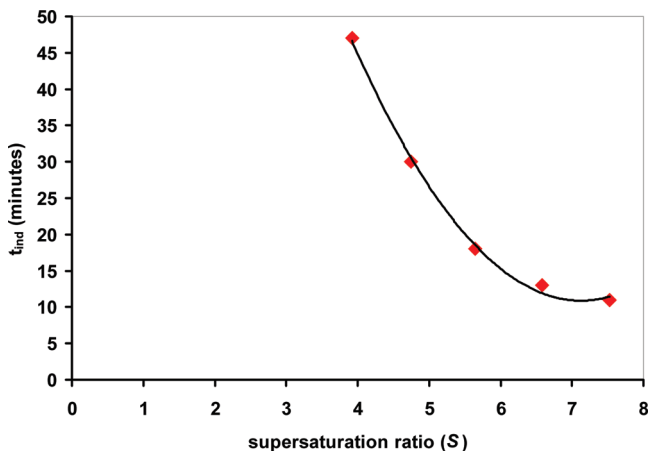


Figure 4. Dependence of the induction time on the supersaturation ratio of gypsum in the presence of 0.05 mg/L EDTMP. The line is drawn to aid the reader.

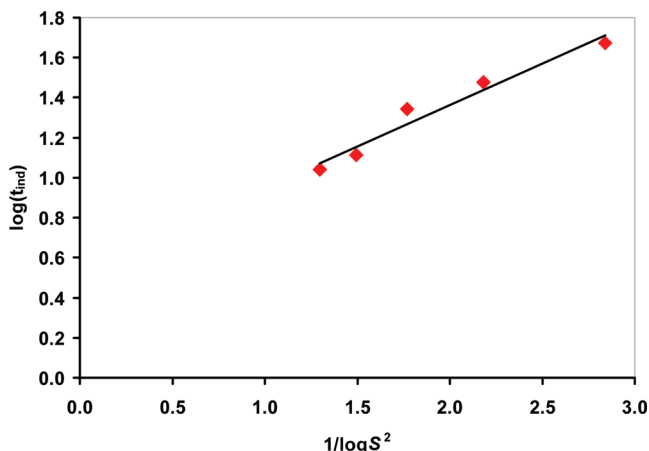


Figure 5. Relation between $\log t_{\text{ind}}$ and $1/(\log \text{supersaturation ratio})^2$ with 0.05 mg/L EDTMP.

They found that the growth followed a second-order parabolic rate law. Attempts to model gypsum precipitation, as discussed above, showed that the reaction rate order seemed to be specific to the experimental system and experimental conditions employed in the study.

Figure 4 shows the dependence of the induction period on the supersaturation ratio for 0.05 mg/L EDTMP concentration. It can be observed that the induction period for gypsum nucleation continuously decreases with an increase in supersaturation.

The dependence of the induction time on temperature and the solution supersaturation, assuming steady state, is given by eq 3,

$$\log t_{\text{ind}} = A + \frac{B}{T^3(\log S)^2} \quad (3)$$

where A and B are constants. B depends on the number of variables and is given by

$$B = \frac{\beta \gamma_s^3 V_m^2}{(2.303k)^3 v^2} \quad (4)$$

where β is a shape factor (taken as $16\pi/3$ here, assuming spherical shape for the nuclei forming), γ_s is the interfacial tension, V_m is the molecular volume, k is Boltzmann's constant, and v is the number of ions in the calcium sulfate crystals ($v = 2$). Plots according to eq 3 are shown in Figure 5.

The interfacial tension between the gypsum crystals and the aqueous solutions is a fundamental parameter for understanding the rate of both nucleation and crystal growth. Relations between t_{ind} and $1/(\log S)^2$ with 0.05 mg/L EDTMP gives a straight line (Figure 5). From the slope of this line, a value of 45 mJ/m^2 of the gypsum overgrowth was estimated.

The values of γ_s in the presence of EDTMP obtained in this work were compared with interfacial tension values for gypsum obtained by different research groups in Table 5. These results taken together with those in Table 2 and Figure 2 confirm that EDTMP is a good retardant for the calcium sulfate crystallization.

Effects of Additives on Calcium Sulfate Dihydrate Crystal Morphology. In this work, phosphonate-based additives were tested for their ability to suppress growth of gypsum by using spontaneous crystallization experiments. The presence of additives in supersaturated solutions affects not only

Table 5. Interfacial Tension Values for Calcium Sulfate Dihydrate in Aqueous Solutions Available in the Literature

additives	concentration (mg/L)	T (°C)	γ_s (mJ/m ²)	ref
blank		30	23.2	Keller et al. (1978), ref 37
amino- <i>tris</i> (methylenephosphonic acid), AMP	5	25	41.2	Prisciandaro et al. (2006), ref 25
amino- <i>tris</i> (methylenephosphonic acid), AMP	10	25	46.5	Prisciandaro et al. (2006), ref 25
amino- <i>tris</i> (methylenephosphonic acid), AMP	50	25	54.0	Prisciandaro et al. (2006), ref 25
citric acid	10	25	37.0	Prisciandaro et al. (2003), ref 38
citric acid	50	25	41.0	Prisciandaro et al. (2003), ref 38
cetyltrimethylammonium bromide	100	80	8.7	Mahmoud et al. (2004), ref 39
sodium dodecyl sulfate	100	80	6.7	Mahmoud et al. (2004), ref 39
ethylenediamine- <i>tetrakis</i> (methylenephosphonic acid), EDTMP	0.05	30	45	this work

Table 6. Comparison of Gypsum Crystal Characteristics Based on SEM Results in the presence of EDTMP

SEM measurement	EDTMP concentration															
	control				2.3×10^{-7} mol/L				3.5×10^{-7} mol/L				5.7×10^{-7} mol/L			
	needle		plate		needle		plate		needle		plate		needle		plate	
size (μm)	W ^a	L ^b	W	L	W	L	W	L	W	L	W	L	W	L	W	L
SD ^c	±0.7	±9.4	±4.8	±13.1	±0.7	±8.6	±2.7	±10.2	±0.7	±5.6	±2.5	±9.7	±0.5	±4.2	±2.2	±8.5

^aW = width. ^bL = length. ^cSD = standard deviation. All dimensions are expressed in μm .

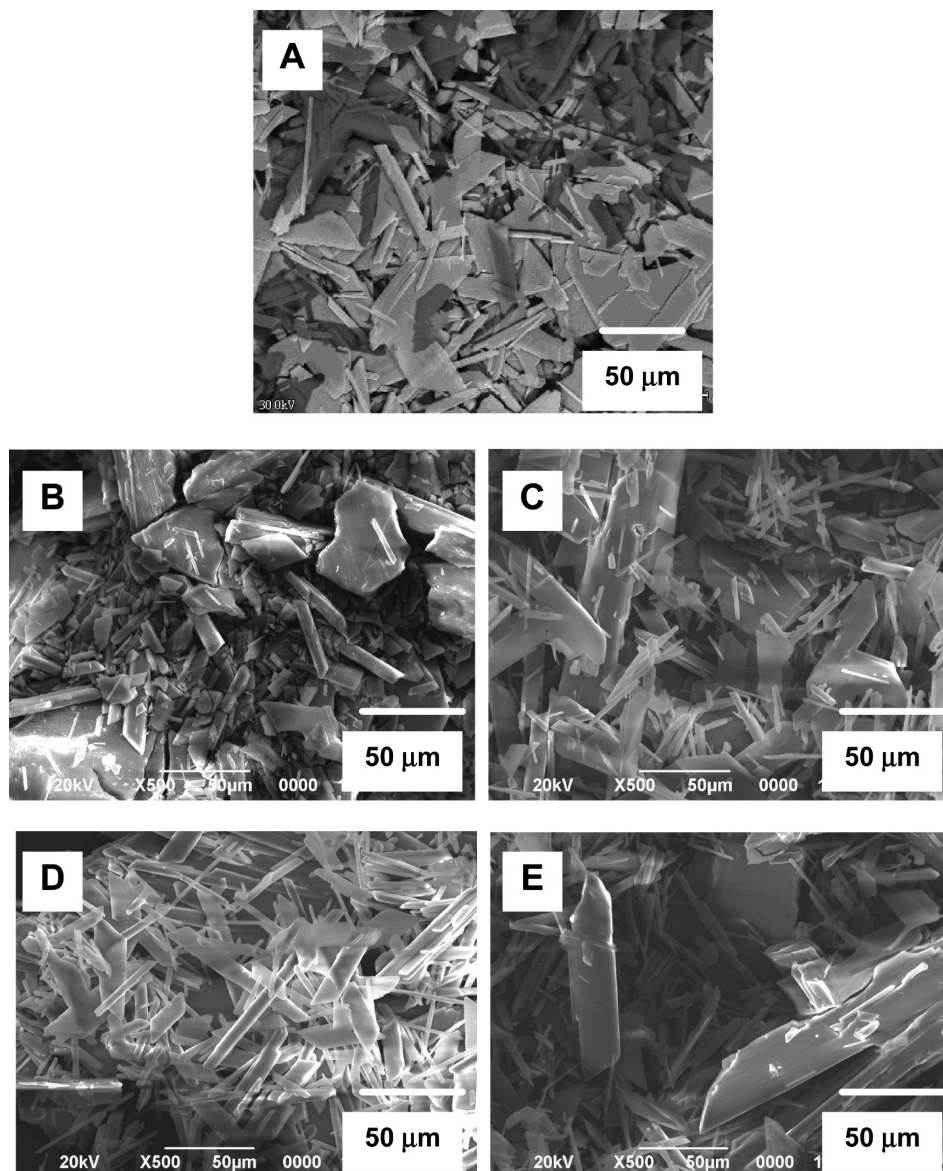


Figure 6. SEM of formed gypsum crystals in the presence of (A) no additives, (B) 0.15 mg/L EDTMP, (C) 0.15 mg/L HDTMP, (D) 0.15 mg/L ODTMP, and (E) 0.15 mg/L DDTMP.

the kinetics of crystal growth but crystal size as well, as shown in Tables 6 and 7. SEM images were collected for subsequent visual analysis in order to assess the effects of additives containing phosphonic acid on crystal morphology (shape and size). The characteristic morphology of gypsum precipitated in the absence of additives is shown Figure 6a. Examination of the morphology of the precipitated gypsum crystals by SEM showed the formation of the characteristic needle-like and plate-like crystals. The crystal habit of the precipitated calcium sulfate crystals was affected by presence of additives, as may be seen in the scanning electron photographs shown in Figure 6b–e. The presence of additives resulted in less elongated needle and plate-like crystals. The length of the needle-like crystals is reduced to $13.9\ \mu\text{m}$ in the presence of $5.7 \times 10^{-7}\ \text{mol/L}$ EDTMP as shown in Table 6.

Crystal sizes of gypsum were also measured by particle sizer. The results are summarized in Table 7. The arithmetic and geometric mean diameters of gypsum crystals are lower with all additives than in the absence additives. The lower mean diameter may indicate that the formed gypsum crystal

growth is lowered compared with the control. The particle sizer results clearly show that DDTMP is the most effective additive because crystals have the smallest size in the presence of DDTMP.

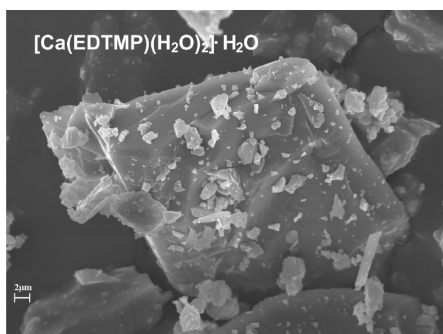
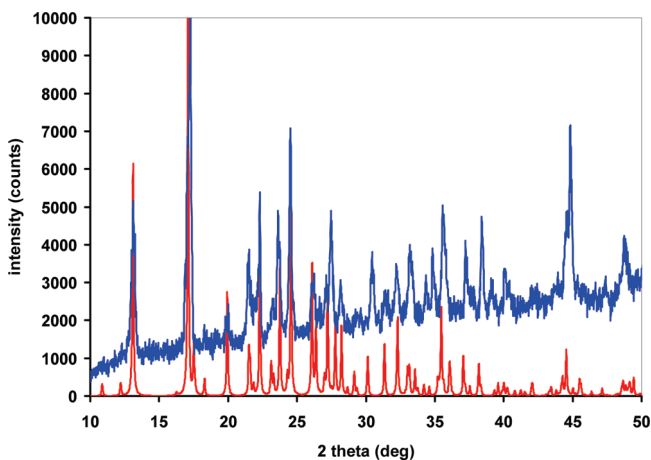
Physicochemical Characterization and Crystal Structure of $[\text{Ca}(\text{EDTMP})(\text{H}_2\text{O})_2] \cdot \text{H}_2\text{O}$. Further insight into the complexation mode of EDTMP with Ca^{2+} in the solid state can be obtained by studying the Ca-EDTMP solids precipitating from the reaction of Ca^{2+} and EDTMP and by examination of the crystal structure of the Ca^{2+} -EDTMP material. The crystals of the Ca-EDTMP coordination polymer are rhombic in their morphology, Figure 7.

The XRD powder pattern of $[\text{Ca}(\text{EDTMP})(\text{H}_2\text{O})_2] \cdot \text{H}_2\text{O}$ solids was measured and compared to the calculated pattern from the crystal structure (vide infra); see Figure 8. The two patterns match well which is proof that the bulk material is identical to that of single crystals.

The crystal structure of the Ca-EDTMP compound reveals an extended, one-dimensional polymer with EDTMP^{2-} acting as both chelating and bridging ligand, Figure 9.

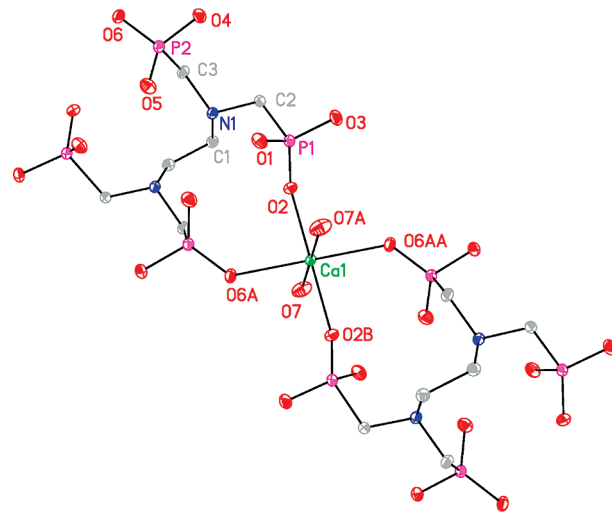
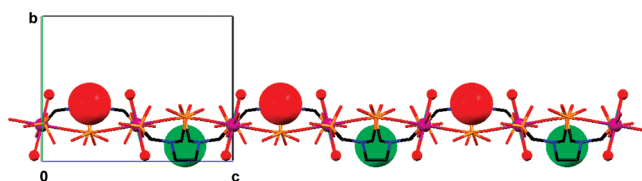
Table 7. Gypsum Particle Size Distribution in the Presence of 0.15 mg/L Tetraphosphonates

diameter (μm)	blank	EDTMP	HDTMP	ODTMP	DDTMP
arithmetic mean (μm)	23.39	21.59	20.84	19.66	17.81
geometric mean (μm)	33.85	33.02	32.09	31.25	27.69
mean square deviation (μm)	13.6	13.6	13.7	13.7	12.1

**Figure 7.** SEM images of single crystals of $[\text{Ca}(\text{EDTMP})(\text{H}_2\text{O})_2] \cdot \text{H}_2\text{O}$.**Figure 8.** Calculated and measured XRD powder patterns of $[\text{Ca}(\text{EDTMP})(\text{H}_2\text{O})_2] \cdot \text{H}_2\text{O}$.

There are some interesting features of the structure. The $-\text{PO}_3\text{H}^-$ group coordinates to Ca^{2+} through only one of its three oxygens. This is in contrast to several literature examples that demonstrate the strong propensity of the $-\text{PO}_3\text{H}^-$ group to bridge two or more metal centers. Two $-\text{PO}_3\text{H}^-$ groups, one from each N, form an 11-membered chelate ring with Ca^{2+} . The same function occurs on the other side of the $-\text{CH}_2\text{CH}_2-$ linker that renders the whole tetraphosphonate a bridge between two Ca^{2+} centers. Thus, one can envision the 1D polymer as a ribbon in a “wave-like” motion composed of Ca-EDTMP-Ca dimers, see Figure 10. Bond distances and angles are presented in Table 8.

The Ca^{2+} is located in a slightly distorted Oh environment shaped by four equatorial phosphonate oxygens and two axial H_2O 's trans to each other. The $\text{Ca}-\text{O}_{(\text{P})}$ bond distances are 2.3325(18) and 2.3507(17) Å, whereas the $\text{Ca}-\text{O}_{\text{water}}$ bond distance is 2.392(2) Å. The water of crystallization rests above a plane formed by four phosphonate oxygens that point toward it. Two of them are protonated forming H-bonds with it. The specific bridging mode of EDTMP observed in the structure of Ca-EDTMP causes the ligand to acquire a strained position. Thus, the $\text{H}_2\text{O}-\text{Ca}-\text{OH}_2$ axial vectors in the dimeric “unit” are not aligned, but form a dihedral angle of

**Figure 9.** Structure of the Ca coordination environment. The equatorial ligands (O2, O6A, O2B, O6AA) are phosphonate oxygens from two different EDTMPs and the axial ones are two water molecules (O7, O7A).**Figure 10.** Wave-like one-dimensional ribbons in the structure of $[\text{Ca}(\text{EDTMP})(\text{H}_2\text{O})_2] \cdot \text{H}_2\text{O}$ viewed along the a -axis. Waters of crystallization are shown as large red and green spheres. Color codes: Ca magenta, P orange, O red, C black, N blue. Hydrogens are omitted for clarity.**Table 8. Selected Bond Distances (Å) and Angles (deg) for $[\text{Ca}(\text{EDTMP})(\text{H}_2\text{O})_2] \cdot \text{H}_2\text{O}$**

bonds		angles	
Ca(1)–O(6)#1	2.3325(18)	O(6)#1–Ca(1)–O(6)#2	180.0
Ca(1)–O(6)#2	2.3325(18)	O(6)#1–Ca(1)–O(2)	92.04(6)
Ca(1)–O(2)	2.3507(17)	O(6)#2–Ca(1)–O(2)	87.96(6)
Ca(1)–O(2)#3	2.3507(17)	O(6)#1–Ca(1)–O(2)#3	87.96(6)
Ca(1)–O(7)#3	2.392(2)	O(6)#2–Ca(1)–O(2)#3	92.04(6)
Ca(1)–O(7)	2.392(2)	O(2)–Ca(1)–O(2)#3	180.0
P(1)–O(2)	1.4967(18)	O(6)#1–Ca(1)–O(7)#3	85.13(8)
P(1)–O(3)	1.5084(18)	O(6)#2–Ca(1)–O(7)#3	94.87(8)
P(1)–O(1)	1.5704(19)	O(2)–Ca(1)–O(7)#3	91.63(7)
P(1)–C(2)	1.811(2)	O(2)#3–Ca(1)–O(7)#3	88.37(7)
P(2)–O(6)	1.4971(18)	O(6)#1–Ca(1)–O(7)	94.87(8)
P(2)–O(5)	1.5074(19)	O(6)#2–Ca(1)–O(7)	85.13(8)
P(2)–O(4)	1.5720(17)	O(2)–Ca(1)–O(7)	88.37(7)
		O(2)#3–Ca(1)–O(7)	91.63(7)
		O(7)#3–Ca(1)–O(7)	180.00(11)

47.18°. Metric features within the EDTMP backbone are virtually the same as those in free EDTMP or its ionic salts.⁴⁰ Only a handful of structurally characterized metal-EDTMP compounds have been reported.⁴¹ The coordination mode of EDTMP is distinctly different in these materials.

Structural Features of Calcium-Phosphonate Binding and Links to Gypsum Inhibition. Examination of the crystal structure of gypsum reveals that Ca^{2+} is 8-coordinated by six sulfate oxygens and two water molecules in a “cis” arrangement, Figure 11.

Therefore, it is reasonable to envision that the interaction of phosphonates with the gypsum surface takes place

through surface complexation by substitution of these water molecules by phosphonate oxygens. In order to map such calcium–phosphonate interactions we have also examined structural features of calcium–phosphonate binding in a number of calcium–tetraphosphonate structures, namely, Ca-EDTMP (this work), Ca-AMP^{2b} (AMP = aminotris(methylenephosphonate)), Ca-HDTMP,⁴² and Ca-ODTMP.⁴³ A common structural feature in these structures is that a chelating ring is formed by the two phosphonate moieties, part of the carbon chain (the amino-bis(methylene) moiety), and the Ca center; see Figure 12. The Ca-EDTMP is a special one because an 11-membered ring forms through Ca–phosphonate interactions from phosphonate groups belonging to two different N atoms. In the other three structures, eight-membered rings are formed through Ca–phosphonate interactions from phosphonate groups belonging to the same N atom. This feature is common in all these structures. The O–Ca–O angle ranges from 86.57° to 87.96°, not far from the H₂O–Ca–H₂O angle of 98.40° in gypsum.

On the basis of the above arguments and assuming that the only interaction between the tetraphosphonates and the gypsum surface is through the amino-bis(methylenephosphonate) moiety of the additives, one would expect that all tetraphosphonate additives (except EDTMP) should exhibit the same or similar inhibition characteristics. However, this is not the case, as discussed in previous sections. Therefore, additional interactions must be occurring. One can envision interactions of an amino-bis(methylenephosphonate) moiety with a calcium ion on the gypsum

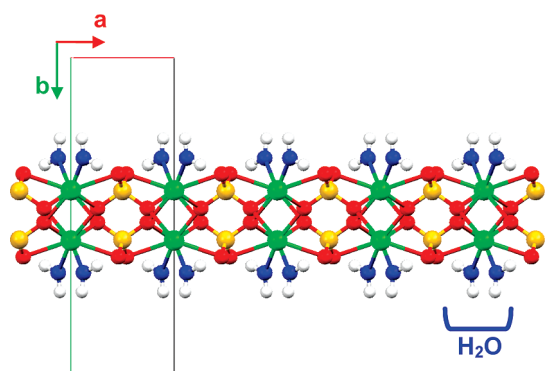


Figure 11. View of the layered portion of the gypsum crystal down the *c*-axis, showing the calcium-coordinated water molecules in blue. Color codes: calcium green, sulfur yellow, oxygen red, hydrogen white.

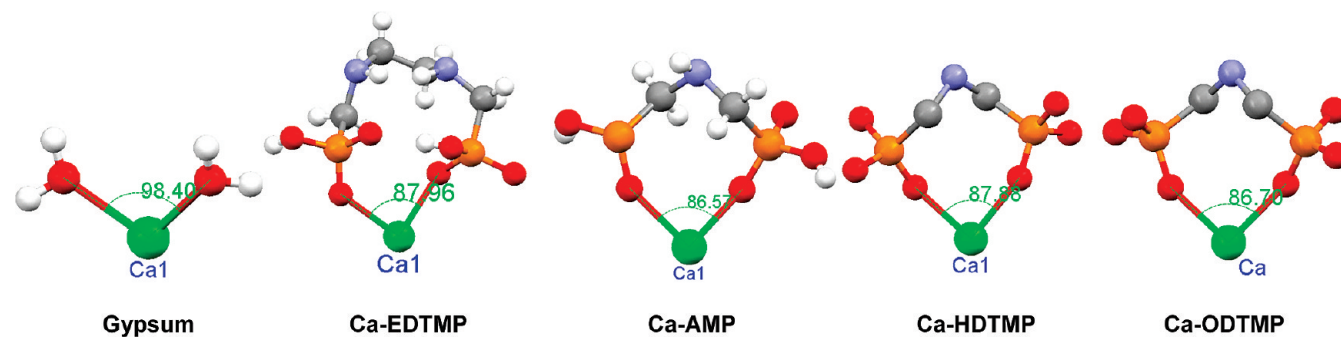


Figure 12. Coordination modes of a bis-phosphonate moiety on calcium, showing the possible replacement of two neighboring water molecules from Ca, in the structure of gypsum.

surface, and, concurrently interaction of the second amino-bis(methylenephosphonate) group with a second, neighboring surface calcium. In gypsum, there are three close Ca neighbors per Ca, one at 5.670 Å and two others at 6.533 and 6.274 Å, all on a plane parallel to the *ac* plane. The question is whether the phosphonate additives have sufficient length to span the appropriate distance, so they interact with two neighboring surface calcium centers. By measuring the longest phosphonate-to-phosphonate O···O distance for each additive (from each “end” of the molecule), the following results are obtained: EDTMP 5.206 Å, HDTMP 8.546 Å, ODTMP 9.724 Å, and DDTMP 16.369 Å. It appears that all additives (except EDTMP) possess sufficient length to span two neighboring calcium ions; therefore, if this argument alone is used to explain the inhibitory activity all additives should be comparable, if not the same. At this point one should invoke possible interactions with surface calcium ions located further away. The distances of the second Ca neighbors are 10.502, 12.548, 13.066 Å. It becomes apparent that only DDTMP is capable of spanning such a long distance, and thus it is the only tetraphosphonate that can participate in such long-range interactions. It should be noted that the polymethylene spacers between the N atoms in the tetraphosphonate backbone allow sufficient flexibility, so “longer” phosphonates may potentially participate in short-range and long-range interactions with surface Ca ions.

One could envision a possible interaction between two phosphonate groups (belonging to the same N atom) with two neighboring calcium ions. The phosphonate-to-phosphonate O···O distances are 3.715 Å for EDTMP, 3.927 Å for HDTMP, 4.247 Å for ODTMP, and 4.219 Å for DDTMP. All are much shorter than the shortest Ca···Ca distances; therefore, this kind of interaction is not likely to occur.

A special note should be made about EDTMP–gypsum interactions. On the basis of the binding mode found in the crystal structure of [Ca(EDTMP)(H₂O)₂]·H₂O and the analysis above, EDTMP can interact with the gypsum surface via two pathways: (a) two phosphonate groups (from two different N atoms) interacting with the same surface Ca²⁺ ion. This chelating mode of binding of EDTMP is the same as that observed in the structure of [Ca(EDTMP)(H₂O)₂]·H₂O. (b) Two phosphonate groups (from two different N atoms) interacting with different (neighboring) surface Ca²⁺ ions. EDTMP possesses sufficient length to achieve such interaction with immediate Ca²⁺ neighboring ions, but not with these located further away, as discussed above. The above interactions are shown schematically in Figure 13.

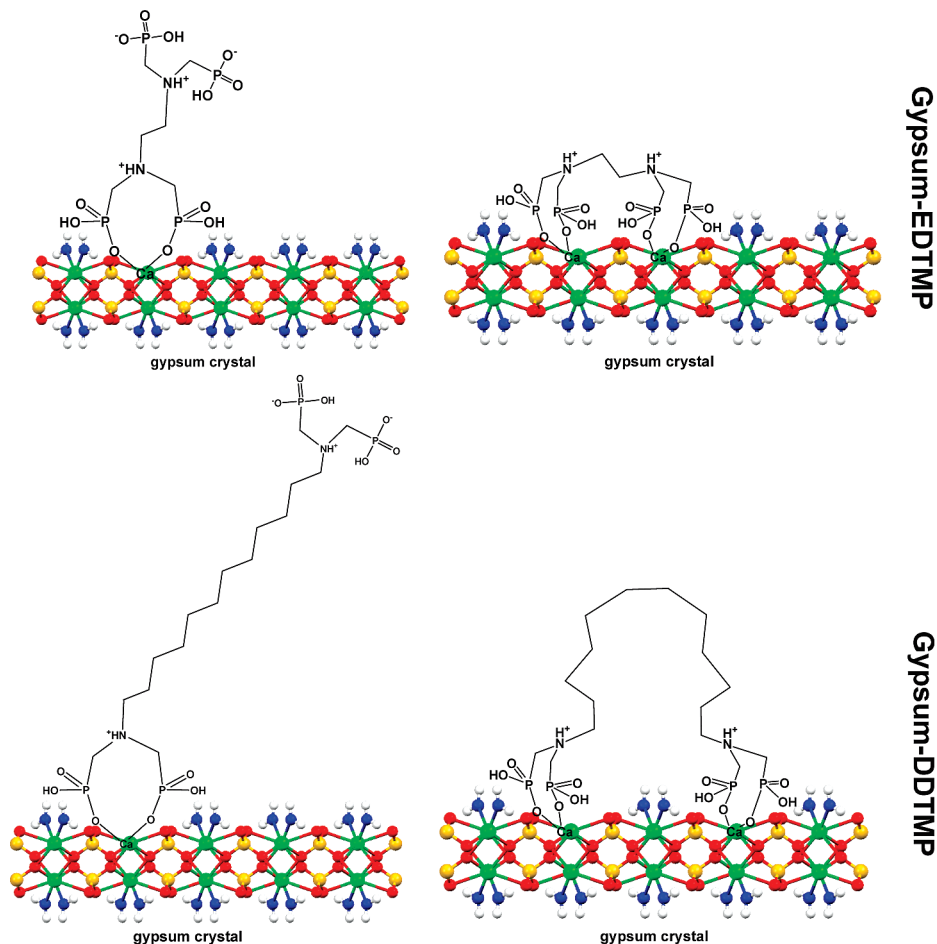


Figure 13. Possible interactions of EDTMP (upper) and DDTMP (lower) with the gypsum surface. Phosphonate structures are schematic and not drawn to scale.

Conclusions

According to these experimental results, all phosphonate additives evaluated in this study strongly affect crystallization rates and crystal sizes and show inhibitory activity for gypsum crystallization. Phosphonate group additives inhibited gypsum precipitation by adsorbing onto crystal surfaces, thus blocking sites for new crystal growth. In the absence of additive, needle- and plate-like particles were obtained. The presence of additives inhibited the crystal growth of gypsum possibly through adsorption onto the active growth sites for crystal growth sites for crystal growth due to their charge and hydrophilic effects. The additive concentration and the degree of supersaturation are found to be important parameters for the control of gypsum crystallization. Possible pathways for growth inhibition are based on the hypothesis that the phosphonate additives interact with surface calcium ions via surface complexation. It was proposed that this occurs by calcium-bound water replacement by the anionic phosphonate oxygen groups.

Acknowledgment. Funding for this work was made possible in the framework of a Bilateral Cooperation Program between Turkey and Greece. M.Ö. thanks the Scientific and Technological Research Council of Turkey (TUBİTAK, Project No: 105M329) and K.D.D. thanks the General Secretariat of Science and Technology (Greece, under contract no. GSRT 2007-202e).

Supporting Information Available: Elemental, spectroscopic and thermogravimetric analyses results, additional structural views, and full structural details for $[\text{Ca}(\text{EDTMP})(\text{H}_2\text{O})_2] \cdot \text{H}_2\text{O}$. Copies of crystallographic data for the structure may be obtained free of charge from CCDC by quoting the reference number 605561. This material is available free of charge via the Internet at <http://pubs.acs.org>.

References

- (1) (a) Uchymiak, M.; Lyster, E.; Glater, J.; Cohen, Y. *J. Membr. Sci.* **2008**, *314*, 163–172. (b) Atamanenko, I.; Kryvoruchko, A.; Yurlova, L.; Tsapiuk, E. *Desalination* **2002**, *147*, 257–262. (c) Alimi, F.; Elfil, H.; Gadri, A. *Desalination* **2003**, *157*, 9–16. (d) Le Gouellec, Y. A.; Elimelech, M. *J. Membr. Sci.* **2002**, *205*, 279–291. (e) Shih, W.-Y.; Rahardianto, A.; Lee, R.-W.; Cohen, Y. *J. Membr. Sci.* **2005**, *252*, 253–263.
- (2) (a) Seewoo, S.; Van Hille, R.; Lewis, A. *Hydrometallurgy* **2004**, *75*, 135–146. (b) Demadis, K. D.; Katarachia, S. D. *Phosphorus, Sulfur Silicon* **2004**, *179*, 627–648. (c) Papadaki, M.; Demadis, K. D. *Comments Inorg. Chem.* **2009**, *30*, 89–118.
- (3) (a) Sweeney, F. M.; Cooper, S. D. Society of Petroleum Engineers International Symposium on Oilfield Chemistry, New Orleans, LA, March 2–5, **1993**; paper SPE 25159. (b) Oddo, J. E.; Tomson, M. B. Corrosion/92; National Association of Corrosion Engineers, Houston, TX, 1992; Paper No. 34. (c) Xiao, J.; Kan, A. T.; Tomson, M. B. *Am Chem. Soc.-Division of Fuel Chemistry, Symposium Preprints* **1998**, *43*, 246–249. (d) Browning, F. H.; Fogler, H. S. *AIChE Journal* **1996**, *42*, 2883–2896. (e) Vetter, O. J. *J. Pet. Tech.* **1973**, *25*, 339–353. (f) Pairat, R.; Sumeath, C.; Browning, F. H.; Fogler, H. S. *Langmuir* **1997**, *13*, 1791–1798. (h) Browning, F. H.; Fogler, H. S. *AIChE J.* **1996**, *42*, 2883–2896.
- (4) (a) El-Shal, H.; Rashad, M. M.; Abdel-Aal, E. A. *Cryst. Res. Technol.* **2002**, *37*, 1264–1273. (b) Rashad, M. M.; Baioumy, H. M.; Abdel-Aal, E. A. *Cryst. Res. Technol.* **2003**, *38*, 433–439.

- (5) Tlili, M. M.; Rousseau, P.; Amor, M. B.; Gabrielli, C. *Chem. Eng. Sci.* **2008**, *63*, 559–566.
- (6) Prisciandaro, M.; Lancia, A.; Musmarra, D. *Ind. Eng. Chem. Res.* **2001**, *40*, 2335–2339.
- (7) Hamdona, S. K.; Al Hadad, O. A. *Desalination* **2008**, *228*, 277–286.
- (8) Lioliou, M. G.; Paraskeva, C. A.; Koutsoukos, P. G.; Payatakes, A. C. *J. Colloid Interface Sci.* **2006**, *303*, 164–170.
- (9) Tadros, M. E.; Mayes, I. *J. Colloid Interface Sci.* **1979**, *72*, 245–254.
- (10) (a) Dogan, Ö.; Akyol, E.; Öner, M. *Cryst. Res. Technol.* **2004**, *39*, 1108–1114. (b) Öner, M.; Doğan, Ö.; Öner, G. *J. Cryst. Growth* **1998**, *186*, 427–437.
- (11) Mwaba, M. G.; Gu, J.; Golriz, M. R. *J. Cryst. Growth* **2007**, *303*, 381–386.
- (12) (a) Cowan, J. C.; Weintritt, D. J. *Water-Formed Scale Deposits*; Gulf Publishing Co.: Houston, TX, 1976. (b) Bott, T. R. *Fouling of Heat Exchangers*; Elsevier Science: Amsterdam, 1995. (c) Demadis, K. D. in *Compact Heat Exchangers and Enhancement Technology for the Process Industries*; Shah, R. K., Ed.; Begell House Inc.: Redding, CT, 2003; pp 483–490. (d) Demadis, K. D.; Lykoudis, P. *Bioinorg. Chem. Appl.* **2005**, *3*, 135–149. (e) Demadis, K. D.; Öner, M. In *Green Chemistry Research Trends*; Pearlman, J. T., Ed.; Nova Science Publishers: New York, 2009; Chapter 8, pp 265–287. (f) Demadis, K. D.; Pachis, K.; Ketsetzi, A.; Stathouloupoulou, A. *Adv. Colloid Interf. Sci.* **2009**, *151*, 33–48. (g) Demadis, K. D.; Neofotistou, E. *Chem. Mater.* **2007**, *19*, 581–587. (h) Demadis, K. D.; Stathouloupoulou, A. *Ind. Eng. Chem. Res.* **2006**, *45*, 4436–4440.
- (13) (a) Amjad, Z. *Mineral Scale Formation and Inhibition*; Plenum Press: New York, 1995. (b) Hulliger, J. *Angew. Chem., Int. Ed.* **1994**, *33*, 143–162. (c) Didymus, J. M.; Oliver, P.; Mann, S.; DeVries, A. L.; Hauschka, P. V.; Westbroek, P. *J. Chem. Soc. Faraday Trans.* **1993**, *89*, 2891–2900.
- (14) (a) Gill, J. S. *Desalination* **1999**, *124*, 43–50. (b) Benton, W. J.; Collins, I. R.; Grimsey, I. M.; Parkinson, G. M.; Rodger, S. A. *Faraday Discuss.* **1993**, *95*, 281–297. (c) Bosbach, D.; Hochella, M. F., Jr. *Chem. Geol.* **1996**, *132*, 227–236. (d) Weijnen, M. P. C.; Van Rosmalen, G. M. *J. Cryst. Growth* **1986**, *79*, 157–168.
- (15) (a) Stamatakis, E.; Chatzichristos, C.; Sagen, J.; Stubos, A. K.; Palyvos, I.; Muller, J.; Stokkan, J.-A. *Chem. Eng. Sci.* **2006**, *61*, 7057–7067. (b) Barouda, E.; Demadis, K. D.; Freeman, S. R.; Jones, F.; Ogden, M. I. *Cryst. Growth Des.* **2007**, *7*, 321–327. (c) Demadis, K. D.; Neofotistou, E.; Mavredaki, E.; Tsiknakis, M.; Sarigiannidou, E.-M.; Katarachia, S. D. *Desalination* **2005**, *179*, 281–295. (d) Bishop, M.; Bott, S. G.; Barron, A. R. *Chem. Mater.* **2003**, *15*, 3074–3088.
- (16) Abdel-Aal, N.; Sawada, K. *J. Cryst. Growth* **2003**, *256*, 188–200.
- (17) Liu, S. T.; Nancollas, G. H. *J. Colloid Interface Sci.* **1975**, *52*, 593–601.
- (18) (a) Lesueur, C.; Pfeffer, M.; Fuerhacker, M. *Chemosphere* **2005**, *59*, 685–691. (b) Dyer, S. J.; Anderson, C. E.; Graham, G. M. *J. Pet. Sci. Eng.* **2004**, *43*, 259–270. (c) Demadis, K. D.; Ketsetzi, A. *Sep. Sci. Technol.* **2007**, *42*, 1639–1649. (d) Demadis, K. D. *Phosphorus Sulfur Silicon* **2006**, *181*, 167–176.
- (19) (a) Mikolajczyk, M.; Balczewski, P. *Top. Curr. Chem.* **2003**, *223*, 162–214. (b) Prinz, E.; Szilágyi, I.; Mogyorósi, K.; Labádi, I. *J. Therm. Anal. Calorim.* **2002**, *69*, 427–439. (c) Carter, R. P.; Carroll, R. L.; Irani, R. R. *Inorg. Chem.* **1967**, *6*, 939–942.
- (20) Kırboğa, S.; Öner, M. *Cryst. Growth Des.* **2009**, *9*, 2159–2167.
- (21) Akyol, E.; Bozkurt, A.; Öner, M. *Polym. Adv. Technol.* **2006**, *17*, 58–65.
- (22) Liu, S. T.; Nancollas, G. H. *Colloid Interface Sci.* **1973**, *44*, 422–429.
- (23) (a) Tomson, M. B.; Kan, A. T.; Fu, G. *SPE J.* **2006**, *11* (3), 283–293. (b) Boak, L. S.; Graham, G. M.; Sorbie, K. S. *Proceedings of the SPE International Symposium on Oilfield Chemistry*; Houston, TX, USA, 1999; pp 643–648. (c) Graham, G. M.; Boak, L. S.; Sorbie, K. S. *SPE Production & Facilities*, February, **2003**; pp 28–44. (d) Graham, G. M.; Boak, L. S.; Sorbie, K. S. *Proceedings of the SPE International Symposium on Oilfield Chemistry*; Houston, TX, USA, 1997; pp 611–626. (e) Sweeney, F. M.; Cooper, S. D. *Proceedings of the SPE International Symposium on Oilfield Chemistry*; New Orleans, LA, USA, 1993; pp 77–89.
- (24) MINEQL+ Chemical Equilibrium Modeling System Ver. 4.0, Hallowell, ME, 1998.
- (25) Prisciandaro, M.; Olivieri, E.; Lancia, A.; Musmarra, D. *Ind. Eng. Chem. Res.* **2006**, *45*, 2070–2076.
- (26) Klepetsanis, P. G.; Koutsoukos, P. G. *J. Cryst. Growth* **1998**, *193*, 156–163.
- (27) Klepetsanis, P. G.; Dalas, E.; Koutsoukos, P. G. *Langmuir* **1999**, *15*, 1534–1540.
- (28) Klepetsanis, P. G.; Koutsoukos, P. G. *J. Colloid Interface Sci.* **1991**, *143*, 299–308.
- (29) Nielsen, A. E. *Kinetics of Precipitation*; Pergamon Press: Oxford, 1964.
- (30) Schierholtz, O. J. *Can. J. Chem.* **1958**, *36*, 1057–1063.
- (31) McCartney, E. R.; Alexander, A. E. *J. Colloid Interface Sci.* **1958**, *13*, 383–396.
- (32) Packter, A. *J. Cryst. Growth* **1974**, *21*, 191–194.
- (33) Nancollas, G. H. *J. Cryst. Growth* **1968**, *3–4*, 335–339.
- (34) Tadros, M. E.; Mayes, I. *J. Colloid Interface Sci.* **1979**, *72*, 245–254.
- (35) Klepetsanis, P. G.; Koutsoukos, P. G. *J. Cryst. Growth* **1989**, *98*, 480–486.
- (36) He, S.; Oddo, J. E.; Thomson, M. B. *J. Colloid Interface Sci.* **1994**, *163*, 372–378.
- (37) Keller, D. M.; Massey, R. E.; Hileman, O. E. *Can. J. Chem.* **1978**, *56*, 831–838.
- (38) Prisciandaro, M.; Lancia, A.; Musmarra, D. *Ind. Eng. Chem. Res.* **2003**, *42*, 6647–6652.
- (39) Mahmoud, M. H. H.; Rashad, M. M.; Ibrahim, I. A.; Abdel-Aal, E. A. *J. Colloid Interface Sci.* **2004**, *270*, 99–105.
- (40) (a) Polyanchuk, G. V.; Shkol'nikova, L. M.; Rudomino, M. V.; Dyatlova, N. M.; Makarevich, S. S. *J. Struct. Chem.* **1985**, *26*, 586–594. (b) Demadis, K. D.; Barouda, E.; Zhao, H.; Raptis, R. G. *Polyhedron* **2009**, *28*, 3361–3367.
- (41) (a) Mondry, A.; Janicki, R. *Dalton Trans.* **2006**, 4702–4710. (b) Janicki, R.; Mondry, A. *Polyhedron* **2008**, *27*, 1942–1946. (c) Wu, J.; Hou, H.; Han, H.; Fan, Y. *Inorg. Chem.* **2007**, *46*, 7960–7970. (d) Demadis, K. D.; Barouda, E.; Stavgiannoudaki, N.; Zhao, H. *Cryst. Growth Des.* **2009**, *9*, 1250–1253.
- (42) Colodrero, R. M. P.; Cabeza, A.; Olivera-Pastor, P.; Infantes-Molina, A.; Barouda, E.; Demadis, K. D.; Aranda, M. A. G. *Chem.—Eur. J.* **2009**, *15*, 6612–6618.
- (43) Cabeza, A.; Aranda, M. A. G., *personal communication*.